

1   **Regulation of synoptic circulation in regional PM<sub>2.5</sub> transport for heavy air pollution:**  
2   **study of 5-year observation over central China**

3   **Weiyang Hu<sup>1</sup>, Tianliang Zhao<sup>1</sup>, Yongqing Bai<sup>2</sup>, Shaofei Kong<sup>3</sup>, Lijuan Shen<sup>1</sup>, Jie Xiong<sup>2</sup>,**  
4   **Yue Zhou<sup>2</sup>, Yao Gu<sup>1</sup>, Junnan Shi<sup>4</sup>, Huang Zheng<sup>3</sup>, and Xiaoyun Sun<sup>1</sup>**

5   <sup>1</sup>Climate and Weather Disasters Collaborative Innovation Center, Key Laboratory for Aerosol-  
6   Cloud-Precipitation of China Meteorological Administration, PREMIC, Nanjing University of  
7   Information Science & Technology, Nanjing, 210044, China.

8   <sup>2</sup>Institute of Heavy Rain, China Meteorological Administration, Wuhan, 430205, China.

9   <sup>3</sup>Department of Atmospheric Sciences, School of Environmental Studies, China University of  
10   Geosciences (Wuhan), Wuhan, 430074, China.

11   <sup>4</sup>Taishan meteorological station of Shandong province, Taishan, 271000, China

12   Corresponding author: T. Zhao (tlzhao@nuist.edu.cn) and Y. Bai (2007byq@163.com)

13

14   **Key Points:**

- 15   • Regional PM<sub>2.5</sub> transport presents an increasing trend over the past 5 years, dominating  
16   heavy pollution events in central China.
- 17   • Three regional transport pathways are identified to central China in the northerly,  
18   northeasterly, and easterly directions respectively.
- 19   • Synoptic circulation modulates regional transport in air quality change with the large  
20   contribution to PM<sub>2.5</sub> over central China.

21

## 22 Abstract

23 The importance of regional air pollutant transport modulated by large-scale synoptic circulation  
24 has been poorly understood for air pollution. In the present study of 5-year (2015-2019)  
25 observation, we targeted the Twain-Hu Basin (THB), a region of heavy PM<sub>2.5</sub> pollution over  
26 central China to investigate the regulation of synoptic circulation governing regional PM<sub>2.5</sub>  
27 transport for heavy air pollution. It was found that regional transport of PM<sub>2.5</sub> predominated  
28 65.2% of the heavy pollution events (HPEs) over the THB based on the statistics of  
29 observational environment and meteorology. By employing the FLEXPART-WRF model, the  
30 regional transport of PM<sub>2.5</sub> from upwind source areas in central and eastern China (CEC) to  
31 receptor region in the THB was identified with three prominent pathways in the northerly,  
32 northeasterly, and easterly directions respectively. Based on T-mode principal component  
33 analysis in conjunction with the K-means cluster method, it was recognized that three regional  
34 PM<sub>2.5</sub> transport pathways for the HPEs over central China were determined respectively by three  
35 patterns of synoptic circulation over CEC with 1) weak high air pressure to the north, 2) strong  
36 high air pressure to the northeast, and 3) weak high air pressure to the east, governing the cold air  
37 invasions southwards to the THB region in central China with the large contributions of 76.0%,  
38 56.7%, and 53.9% to the THB- PM<sub>2.5</sub> concentrations in the HPEs, revealing a significant  
39 modulation of large-scale synoptic circulation for regional transport of air pollutants in  
40 environmental change.

## 41 1 Introduction

42 PM<sub>2.5</sub> pollution has aroused worldwide attention owing to its adverse effects on human  
43 health (Agarwal et al., 2017; Dang and Liao, 2019), atmospheric visibility (Wang et al., 2020),  
44 and direct and indirect impacts on weather and climate (Bi et al., 2016; Zhou et al., 2017; Che et  
45 al., 2019). In recent years, high PM<sub>2.5</sub> levels in the ambient atmosphere during heavy air  
46 pollution events have occurred across central and eastern China (CEC), even though the Chinese  
47 government has enacted stringent and effective measures to mitigate air pollution, such as the  
48 national-scale Air Pollution Prevention and Control Action Plan (Clean Air Plan) in 2013 (China  
49 State Council, 2013). Comprehensively understanding the underlying mechanism for frequent  
50 heavy air pollution events is of vital importance for improving air quality.

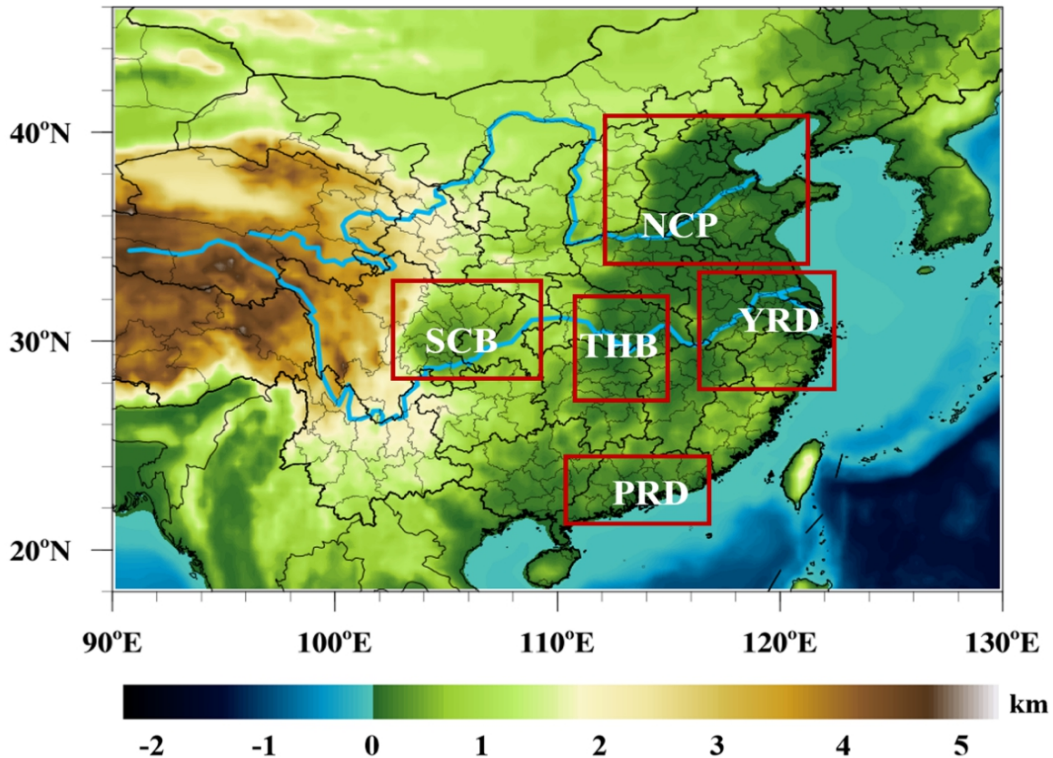
51 Excessive air pollutant emissions are the primary cause of atmospheric pollution (Su et al.,  
52 2019., Zhang et al., 2020). After the Clean Air Plan implementation, air pollution in China

53 mitigated remarkably due to the effective reductions of SO<sub>2</sub>, CO, NOx, PM<sub>10</sub> and primary PM<sub>2.5</sub>  
54 (Fan et al., 2020; Gui et al., 2019; K. Zhang et al., 2019; Zhong et al., 2018). In addition to air  
55 pollutant emissions, meteorological conditions play critical roles in controlling the evolution of  
56 air pollution events (Chen et al., 2018; Shen et al., 2020a; Zhang et al., 2013; Zhang et al., 2015).  
57 Generally, air stagnant conditions of meteorology with weak or calm winds, near-surface thermal  
58 inversion layer, and steady atmospheric boundary layers, can impede air pollution dissipation,  
59 reinforcing air pollutant accumulations (Chen et al., 2017; Guo et al., 2017; Li et al., 2019; Ren  
60 et al., 2017; Zhu et al., 2018). Furthermore, driven by strong winds in multi-scale atmospheric  
61 circulations, air pollutants transported from air pollutant source regions can result in  
62 deteriorating air quality over the downwind receptor regions, which is a complicated issue in  
63 atmospheric environment (Hu et al., 2018; Hu et al., 2021; Huang et al., 2020; Yu et al., 2020).

64 Meteorological conditions are largely connected with large-scale synoptic circulations.  
65 Previous studies have indicated the relationship of air pollution with synoptic circulation in  
66 different areas by using circulation-based classification methods, which suggests that synoptic  
67 patterns are a key driver of air quality variations (Bei et al., 2016, 2020; Comrie & Yarnal, 1992;  
68 Demuzere et al., 2009; He et al., 2016, 2017a; Kalkstein & Corrigan, 1986; Li et al., 2019; Lu et  
69 al., 2021; Shahgedanova et al., 1998). For instance, six types of synoptic circulation were  
70 identified for wintertime air pollution over North China Plain (NCP) from 2013 to 2018, two of  
71 which are prone to outward transport of local PM<sub>2.5</sub> due to the unstable atmospheric stratification,  
72 while the other four types, because of the air stagnation conditions, can elevate local air pollution  
73 levels (Wang and Zhang, 2020). Atmospheric circulations can affect air pollution in the Yangtze  
74 River Delta (YRD) over eastern China with the southward movement of strong cold air, easterly  
75 wind removal, and strong precipitation washout respectively (Hou et al., 2020). Three typical  
76 patterns of synoptic circulation including the dry low-trough, high-pressure, and wet low-vortex,  
77 were associated respectively with heavy, medium, and slight levels of air pollution determining  
78 air quality over the Sichuan Basin (SCB) in southwestern China (Ning et al., 2019). The  
79 variations in PM<sub>2.5</sub> over the Pearl River Delta (PRD) were also connected with different synoptic  
80 patterns in southern China (Liao et al., 2020; Liu et al., 2020). However, the driving effect of  
81 synoptic circulation on regional transport of PM<sub>2.5</sub> in heavy air pollution has been poorly  
82 understood. Furthermore, how regional PM<sub>2.5</sub> transport pathways regulated by synoptic

83 circulation was also lack of exploration. A comprehensive understanding of these issues could be  
84 helpful for improving air quality.

85 The Twain-Hu Basin (THB) covers the flat lands over Hubei and Hunan provinces in the  
86 middle basin of the Yangtze River over central China (Fig. 1). The THB is a region with heavy  
87 air pollution featured by high PM<sub>2.5</sub> levels over central China, especially during the season of  
88 East Asian winter monsoon (Shen et al., 2020b; Zhu et al., 2021). Due to the East Asian winter  
89 monsoons' prevailing winds, regional transport of PM<sub>2.5</sub> plays a dominant part in a heavy air  
90 pollution period in central China with transport contribution of 70.5% (Hu et al., 2021). Although  
91 the dominant synoptic patterns were classified for heavy pollution of PM<sub>2.5</sub> in the region of THB  
92 over central China from 2013 to 2018 (Yan et al., 2020), few studies have analyzed the  
93 modulation of synoptic circulation on regional PM<sub>2.5</sub> transport for heavy PM<sub>2.5</sub> pollution in  
94 central China, given that the THB is a key receptor region in regional air pollutant transport over  
95 CEC because of its special geographical position with a typical East Asian winter monsoon  
96 climate (Yu et al., 2020).



97

98 **Figure 1.** The geographical location of THB, North China Plain (NCP), Yangtze River Delta (YRD), Pearl  
 99 River Delta (PRD) and Sichuan Basin (SCB) over CEC with the terrain height (km in a.s.l.; shaded contours)  
 100 from the 2-Minute Gridded Global Relief Data (ETOPO2v2)  
 101 (<http://www.ngdc.noaa.gov/mgg/global/etopo2.html>). Two blue lines respectively indicate the Yellow River  
 102 and Yangtze River in China.

103

104 In this study, we characterized the heavy air pollution events (HPEs) affected by regional  
 105 transport of PM<sub>2.5</sub> in the THB in central China based on statistics of observation from 2015 to  
 106 2019. By using FLEXPART-WRF modeling, we identified three prominent regional PM<sub>2.5</sub>  
 107 transport pathways with the contributions to PM<sub>2.5</sub> concentrations for the HPEs over central  
 108 China. Besides, we detected the large-scale synoptic systems in regional PM<sub>2.5</sub> transport through  
 109 the T-mode principal component analysis (T-PCA) combined with the K-means cluster method  
 110 and ascertained the regulation of synoptic circulation patterns in three regional PM<sub>2.5</sub> transport  
 111 pathways dominating HPEs in central China. We also estimated the regional PM<sub>2.5</sub> transport's  
 112 contribution in three major pathways to PM<sub>2.5</sub> concentrations of the HPEs under different types

113 of synoptic circulation. This study aimed to understand the modulation of large-scale  
114 atmospheric circulation for regional transport of air pollutants in environmental change.

115 **2 Data and methods**

116 **2.1 PM<sub>2.5</sub> and meteorological data sources**

117 We used hourly surface PM<sub>2.5</sub> concentration data observed over CEC over 2015-2019 in this  
118 study, which were derived from the National Air Quality Monitoring Network operated by the  
119 Ministry of Ecology and Environment of China (<http://106.37.208.233:20035/>).

120 The data of sea level pressure (SLP), air temperature and u-, v-, and w-wind components  
121 with  $0.25 \times 0.25^\circ$  resolution during 2015-2019 were obtained from the ERA5 meteorological  
122 reanalysis data of the ECMWF. Moreover, the 5-year observational meteorological data,  
123 including near-surface air temperature, relative humidity, SLP, wind speed, wind direction, and  
124 precipitation, with 1h temporal resolution, were downloaded from the China meteorological data  
125 service center of China Meteorological Administration (<http://data.cma.cn/>).

126 **2.2 Synoptic circulation classification**

127 T-mode principal component analysis (T-PCA) combined with the K-means cluster was  
128 applied to classify the synoptic circulation types for the HPEs in the THB receptor region in  
129 regional PM<sub>2.5</sub> transport over CEC. T-PCA combined with K-means clustering has been widely  
130 used in previous studies on environmental change with the reasonable performance in identifying  
131 synoptic circulations (Huth, 1996, 2008; He et al., 2017, 2018; Liu et al., 2020; Miao et al., 2017;  
132 Zhang et al., 2012).

133 Three processing steps were used to classify the types of synoptic circulation. First, three-  
134 dimensional SLP, were reshaped to two-dimensional dataset (grid  $\times$  time) and standardized  
135 thereafter. Second, the normalized data applying T-PCA with the major components were  
136 acquired according to a cumulative variance contribution of 84.0%. Third, through K-means  
137 clustering, the main components were selected based on the cluster results. The number of  
138 synoptic circulation type classifications relies on the criterion function (Liu and Gao, 2011).  
139 Finally, three types of synoptic circulation for regional PM<sub>2.5</sub> transport for HPEs were  
140 ascertained.

141 The study domain over 20–50° N and 100–130° E in east and north Asian regions includes  
142 mainland China and most Mongolian areas. The daily mean SLP data from ERA5 was used to

143 eliminate the biases caused by local small-scale atmospheric circulation, such as land and sea  
144 breezes (Hou et al., 2020).

145 **2.3 FLEXPART-WRF model and configuration**

146 The FLEXPART (Stohl et al., 2005; Fast and Easter, 2006), a Lagrangian transport and  
147 dispersion model, considering atmospheric physicochemical processes i.e., tracer regional  
148 transport, wet and dry depositions, turbulent diffusion (Brioude et al., 2013), was applied in this  
149 study to backwards trace the released particle trajectory arriving at the receptor region, further  
150 verifying the corresponding air pollutant transport patterns and the spatial distribution of air  
151 pollutant source areas that may affect the receptor site.

152 The WRF model output of meteorology was used to drive the FLEXPART (Skamarock et  
153 al., 2008). The NCEP FNL reanalysis data in the horizontal resolution of  $1 \times 1^\circ$  were applied to  
154 provide the initial and boundary conditions for the WRF modeling. The physical process  
155 parameterization schemes used in the WRF-simulations included the Lin for microphysics  
156 scheme (Lin et al., 1983), RRTM (Mlawer et al., 1997) for long-wave radiation scheme, Goddard  
157 (Chou et al., 1999) for short-wave radiation scheme, and YSU scheme (Hong et al., 2006) of the  
158 planetary boundary layer (PBL) processes. More details of the WRF model configuration can be  
159 found in Table S1.

160 A 48-h backward trajectory was conducted by FLEXPART-WRF simulation, which  
161 released 50000 computational air particles with  $0.1 \times 0.1^\circ$  horizontal resolution, centered at a  
162 representative THB-site ( $32.04^\circ$  N,  $112.14^\circ$  E), namely Xiangyang, for the wintertime HPEs  
163 from 2015 to 2019.

164 **2.4 WRF-Modeling validation**

165 The validation of the WRF modeling results with observation of air temperature, wind  
166 speed, air pressure, and relative humidity, at the sites Xiangyang, Zhengzhou, Changsha, Hefei,  
167 and Nanchang in CEC is shown in Figure S1. The positive correlation coefficients passing the  
168 0.002 significance level and the low normalized standardized deviations were proved to be  
169 reasonable in the WRF-modeling, indicating that the meteorology of fine WRF simulation could  
170 be used to drive the FLEXPART modeling on the routes of regional air pollutant transport with  
171 the contribution to PM<sub>2.5</sub> concentrations for heavy air pollution in central China.

172 **2.5 Assessment on regional PM<sub>2.5</sub> transport contribution**

173 Regional PM<sub>2.5</sub> transport to the receptor region was assessed with the contribution by  
 174 multiplying the primary PM<sub>2.5</sub> emission flux by the residential time of air particles from the 48 h  
 175 backward trajectory simulations of the FLEXPART-WRF, and regional PM<sub>2.5</sub> transport pathway  
 176 over CEC could be identified with the spatial distribution of high contribution rate<sub>i,j</sub> in the  
 177 following Eq.(1):

$$\text{Contribution rate}_{i,j} = \frac{E_{i,j} \times r_{i,j}}{\sum_{1,1}^{N,S} E_{i,j} \times r_{i,j}} \quad (1)$$

178 where i and j stand for the grid location (*i, j*) from the first grid cell (*i*=1, *j*=1) to the last grid cell  
 179 (*j*=*N*, *j*=*S*) over CEC on the 48-h backward trajectory, *r<sub>i,j</sub>* means PM<sub>2.5</sub> residential time from the  
 180 FLEXPART-WRF simulation, and *E<sub>i,j</sub>* manifests the PM<sub>2.5</sub> emission intensity over the grid at  
 181 location (*i, j*) from the Multi-resolution Emission Inventory for China (MEIC;  
 182 <http://www.meicmodel.org/>).

$$R = \sum_{(N_1, S_1)}^{(N_2, S_2)} \text{rate}_{i,j} \quad (2)$$

183 R means the total contribution of regional transport of PM<sub>2.5</sub> from the external regions over the  
 184 first and last grid cells respectively at (*N*<sub>1</sub>, *S*<sub>1</sub>) and (*N*<sub>2</sub>, *S*<sub>2</sub>) over the non-local emission sources to  
 185 the HPEs in the THB receptor region over central China through the FLEXPART-WRF  
 186 simulation (Yu et al., 2020 ; Chen et al.,2017).

187 **3 Results and Discussion**

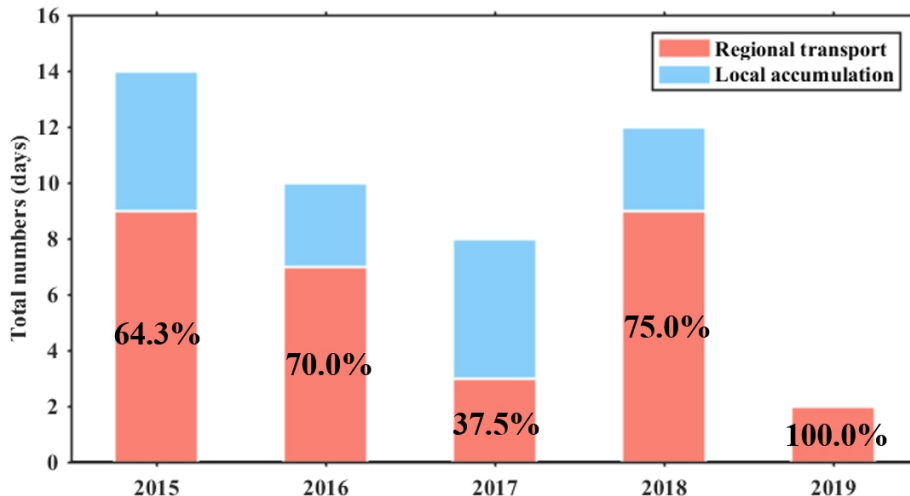
188 **3.1 Regional transport of PM<sub>2.5</sub> dominating heavy air pollution**

189 Firstly, 46 days of regional HPEs over the THB from 2015 to 2019 were detected with the  
 190 daily averaged surface PM<sub>2.5</sub> concentrations greater or equal than 150 µg m<sup>-3</sup> observed at three or  
 191 more sites, which all happened in the East Asian winter monsoon season from November to  
 192 following March (Table S2), reflecting a close linkage of the seasonal shift of East Asian  
 193 monsoons with regional change of atmospheric environment. Then, based on the climatology of  
 194 cold air invasion with southward advance of high air pressure system from northern China  
 195 triggered by East Asian winter monsoonal winds (Ding, 1993; Hou et al., 2020; Wang et al.,  
 196 2020), we established the criterion for wintertime regional transport of air pollutants to the THB  
 197 with the sea level pressure gradient (> 3.0 hPa) between 33° N and 26° N averaged over 112° E-

198 114° E and the regional average meridional component ( $< -1.0 \text{ m s}^{-1}$ ) of near-surface wind.  
199 According to this criterion, 30 days of HPEs in central China connecting with regional transport  
200 of PM<sub>2.5</sub> were selected out among the 46 days of regional HPEs based on the statistics of  
201 observed HPEs over 2015-2019. Therefore, it was estimated with the ratio of 30/46 days of  
202 regional HPEs that 65.2% of the HPEs in the THB during the recent 5 years were influenced by  
203 the regional PM<sub>2.5</sub> transport with strong near-surface northerly (meridional) winds.

204 Generally, air pollution is formed by local accumulation and regional air pollutant transport  
205 (Chen et al., 2017; Yu et al., 2020; Zhu et al., 2018). Figure 2 displays the proportion (%) of the  
206 HPEs affected by regional PM<sub>2.5</sub> transport during total HPEs for assessing the impacts of  
207 regional transport and local accumulation on the change of HPEs over the THB from 2015 to  
208 2019. The HPEs influenced with regional PM<sub>2.5</sub> transport were accounted for 64.3%, 70.0%,  
209 37.5%, 75.0%, and 100.0% over 2015-2019 (Fig. 2), presenting an increasing trend in the  
210 dominant contribution of regional transport of PM<sub>2.5</sub> to the HPEs over the recent years, which is  
211 distinguished from the local accumulation of air pollutants under the stagnant air conditions  
212 causing the HPEs in most regions over CEC (Cai et al., 2017; Shu et al., 2021; Zhang et al., 2018;  
213 Zhong et al., 2019).

214



215

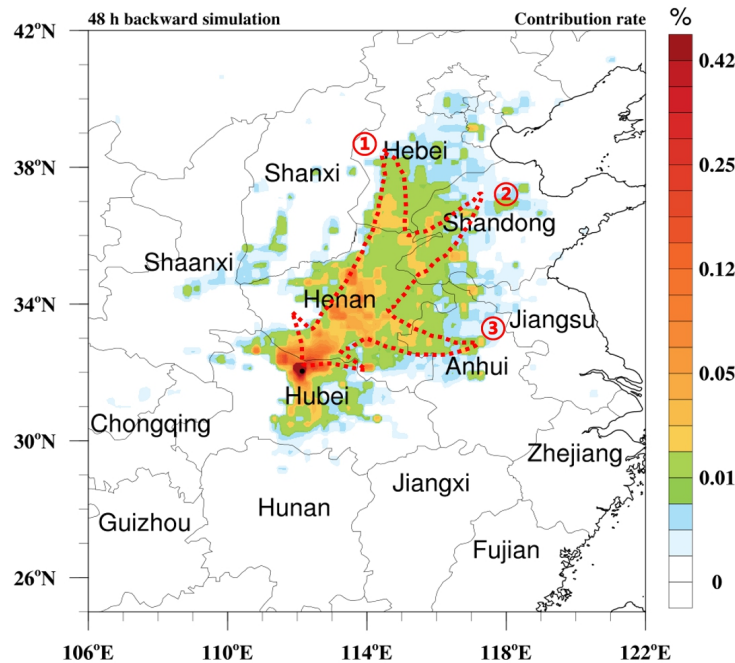
216 **Figure 2.** Annual occurrence days of regional transport (red column) and local accumulation (blue column) in  
 217 the regional HPEs over the THB in central China from 2015 to 2019. The percentages mean the proportion of  
 218 HPEs dominated with regional PM<sub>2.5</sub> transport.

219     3.2 Identifying pathways and contribution of regional transport

220     In section 3.1, we found the dominance of regional transport of PM<sub>2.5</sub> during the HPEs  
 221 based on the statistics of observation over the THB from 2015 to 2019. In this section, the  
 222 pathways of regional PM<sub>2.5</sub> transport from upwind areas to the THB in central China were  
 223 recognized with quantifying the corresponding contribution to the HPEs through the residence  
 224 time of air particle tracer simulated by the FLEAXPART-WRF and the PM<sub>2.5</sub> emission flux over  
 225 the air pollutant sources in CEC with Eqs. (1) and (2).

226     The major pathways of regional transport to the downwind receptor region could be  
 227 identified with high contribution rates of regional transport to PM<sub>2.5</sub> pollution events (Yu et al.,  
 228 2020). Figure 3 displays the average distribution of regional transport pathways with high PM<sub>2.5</sub>  
 229 contribution rates of sources to the THB in central China for 30 days of regional HPEs from  
 230 2015 to 2019. It was recognized from Figure 3 that PM<sub>2.5</sub> from regional transport to the THB-  
 231 region during the HPEs is climatologically centered on three typical transport routes in the  
 232 northerly, northeasterly, and easterly transport directions, respectively. Furthermore, the  
 233 dominant PM<sub>2.5</sub> contribution of regional transport emitted from non-local regions over CEC to  
 234 PM<sub>2.5</sub> concentrations for HPEs in the THB in central China from 2015 to 2019 was averaged as  
 235 60.2% (Table S3), revealing a determining part of PM<sub>2.5</sub> transported from the upwind source  
 236 areas in worsening air environment over central China from a long-term perspective.

237



238

239 **Figure 3.** Distribution of averaged contribution rates (color contours) to surface PM<sub>2.5</sub> during 30 heavy  
 240 pollution days in the THB from 2015 to 2019 with three dominant regional PM<sub>2.5</sub> transport pathways (red  
 241 dashed arrows) in the (1) northerly, (2) northeasterly and (3) easterly directions over CEC.

242

243 Since the synoptic circulation exert a strong influence on PM<sub>2.5</sub> concentrations over CEC  
 244 (He et al., 2017a; He et al., 2017b; He et al., 2018; Zong et al., 2021), the regulation of synoptic  
 245 circulation on building the three routes of regional transport from the upwind sources over CEC  
 246 to central China for the downwind regional HPEs (Fig. 3), require an in-depth exploration to  
 247 improve the understanding in air quality change.

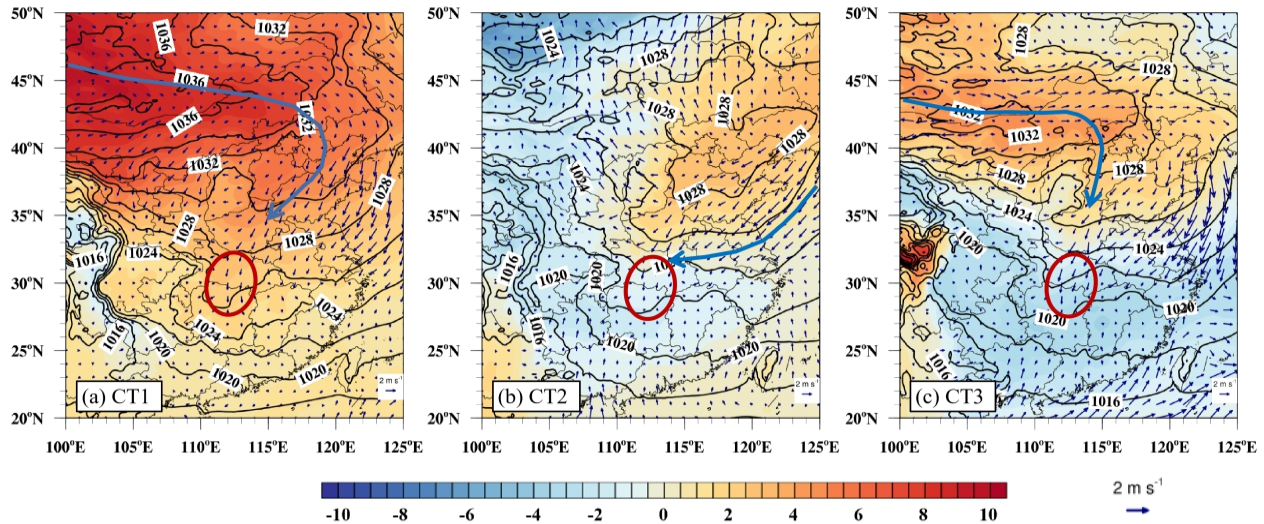
### 248 3.3 Synoptic circulation in regional PM<sub>2.5</sub> transport to HPEs

249 The T-PCA combined with K-means cluster classification was applied to the HPEs with  
 250 regional PM<sub>2.5</sub> transport, and three dominant synoptic circulation types were identified (Table  
 251 S4). Figure 4 shows the anomalous patterns of sea level pressure (SLP) in three dominant  
 252 synoptic circulation types. As the typical feature of East Asian winter monsoon, the cold air  
 253 masses sweep across CEC with the southward advance of high-pressure system, whose shifting  
 254 location and intensity alter the weather process and meteorological elements (Ding, 1993; Ding

255 et al., 2017). According to the location and intensity of high-pressure systems over CEC with  
256 cold air southward invasion driving regional PM<sub>2.5</sub> transport to the THB for the HPEs, three  
257 dominant synoptic patterns were described as strong high pressure to the northeast (CT1), weak  
258 high pressure to the east (CT2), and weak high pressure to the north (CT3).

259 The synoptic circulation type CT1 was the most frequent, accounting for 46.7% of the total  
260 synoptic circulation. For CT1, a strong high-pressure system originating in the Siberian region  
261 extended from Mongolia to China (Fig. S3). In this pattern, northeasterly wind anomalies  
262 prevailed in northern China (NC) and changed to northerly winds into the THB over central  
263 China (Fig. 4a) accompanied by the negative anomalies of air temperature in the vertical layers  
264 for the strong cold air invasion (Fig. S2a), with wind speed of 2.6 m s<sup>-1</sup> (Table S5), transporting  
265 air pollutants from NC to the THB. The CT2 occurrence frequency was 40.0%. In CT2, a weak  
266 surface air pressure with anticyclone was situated northeasterly to the THB over China (Fig. 4b),  
267 which was nearly controlled by the warm air mass anomalies (Fig. S2b) with the 2-m air  
268 temperature increasing up to 7.4 °C (Table S5). In this pattern, the prevailing easterly winds  
269 cover east China with the average wind speed of 2.7 m s<sup>-1</sup> (Table S5) in the THB, which is  
270 conducive to bringing air pollutants from eastern China, mainly the YRD to the THB. The CT3,  
271 from Mongolia region to northern China (Fig. S4) was the relatively week high-pressure system  
272 differing from the CT1 (Figs. 4c and 5c) with 3.1 m s<sup>-1</sup> averaged wind speed over the THB in the  
273 north direction (Table S5), strengthening PM<sub>2.5</sub> transport from non-local source areas to the THB  
274 for the HPEs.

275



276

277 **Figure 4.** The average daily SLP (black lines; hPa) and 10-m wind vector anomalies ( $\text{m s}^{-1}$ ) in the three  
 278 synoptic circulation patterns (a) CT1, (b) CT2 and (c) CT3 for the wintertime HPEs dominated by regional  
 279 PM<sub>2.5</sub> transport from 2015 to 2019 with the anomalies of daily SLP (color contours; hPa) over CEC. The wind  
 280 (SLP) anomalies were relatively with the 5-year wintertime mean of winds (SLP). Blue thick lines with arrows  
 281 mean the dominant southward routes of cold air invasions, and red circles roughly outline the THB areas in  
 282 central China.

### 283 3.4 Modulation of synoptic circulation on regional transport of PM<sub>2.5</sub>

284 Aiming to explore the modulation of synoptic circulation on PM<sub>2.5</sub> from regional transport  
 285 to the HPEs over central China, we investigated the synoptic circulation evolution affected PM<sub>2.5</sub>  
 286 transported from upwind areas over CEC to the THB. Figure 5 exhibits the evolution of three  
 287 synoptic circulations and the changes in PM<sub>2.5</sub> concentrations during the regional transport of  
 288 PM<sub>2.5</sub> over CEC. It shows that synoptic circulation evolution with different location and intensity  
 289 of advancing high air pressure in anticyclone could build three routes of regional PM<sub>2.5</sub> transport  
 290 from the upwind source regions to downwind regional HPEs in CEC (Fig. 5).

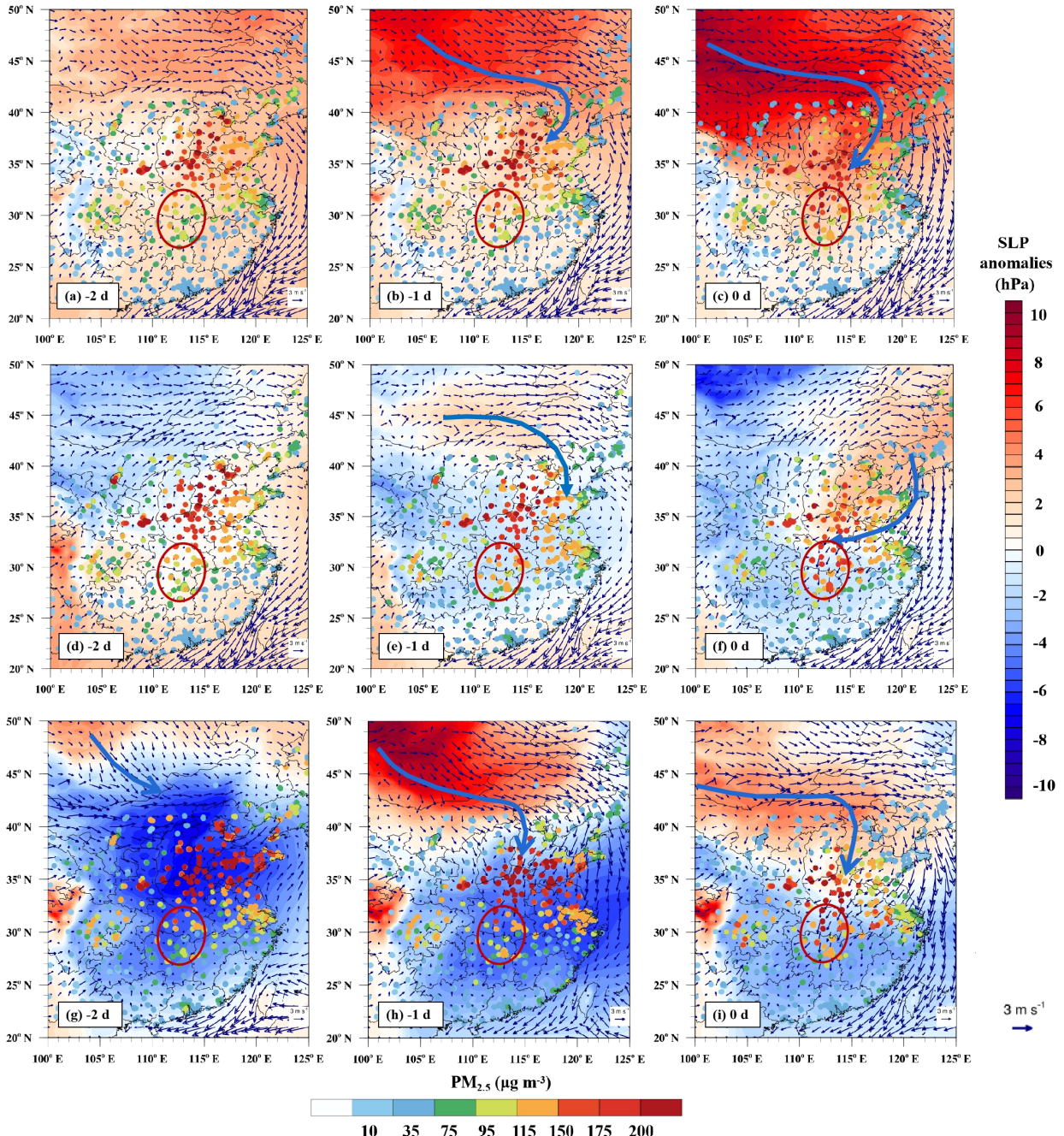
291 In CT1, the positive SLP anomalies existed over the northern CEC. In the beginning of the  
 292 THB's heavy air pollution, weak winds engendered the air pollutant accumulations over the  
 293 northern CEC with high surface PM<sub>2.5</sub> levels over the NCP (Fig. 5a). At the developing stage  
 294 (Fig. 5b), as the relatively strong cold air mass from Mongolia moved southwards, weak winds  
 295 gradually turned into strong northeasterly wind fields over the northern CEC. With the  
 296 southward advance of cold air mass, high PM<sub>2.5</sub> concentrations from the upstream areas over

297 CEC were transported to the downwind regions, mainly the THB, and PM<sub>2.5</sub> concentrations over  
298 the NCP significantly decreased (Fig. 5c).

299 With CT2, the weak high-pressure anomalies moved southeastwards over CEC with  
300 prevailing northerly and northwesterly winds, leading to PM<sub>2.5</sub> transport to the downstream areas  
301 (Figs. 6d-6e). On the day of heavy air pollution in the THB, the high pressure was shifted in the  
302 southeast direction and finally covered northeastern China with obvious northeasterly winds over  
303 the YRD. PM<sub>2.5</sub>, therefore, was transported finally to the THB in the easterly winds over central  
304 China (Fig. 5f).

305 During CT3, there was an apparent low-pressure system occupied over CEC 1-2 days  
306 before the HPEs over the THB (Figs. 6g and 6h). The air pollution levels over the NCP in the  
307 northern CEC were the most serious among three synoptic circulation types (Figs. 6h and 6g). A  
308 strong cold air mass moved southward from Mongolia to NCP, driving PM<sub>2.5</sub> from the NCP to  
309 the downstream areas (Fig. 5h), PM<sub>2.5</sub> parcels over the NCP were transported to the THB by the  
310 prevailing northerly winds in the CT3 (Fig. 5i).

311



312

313 **Figure 5.** Spatial distribution of 10-m wind vectors ( $\text{m s}^{-1}$ ), SLP anomalies (hPa; color contours) and  
 314 PM<sub>2.5</sub> concentrations ( $\mu\text{g m}^{-3}$ ; color dots) at (a, d, g) 2 days and (b, e, h) 1 day before the HPEs as well as  
 315 (c, f, i) at the day of HPEs dominated with regional PM<sub>2.5</sub> transport over CEC. Blue thick lines with arrows mean  
 316 the dominant routes of cold air southward invasions, and a-c, d-f, and g-i represent the evolution of synoptic  
 317 circulation types CT1, CT2, and CT3, respectively.

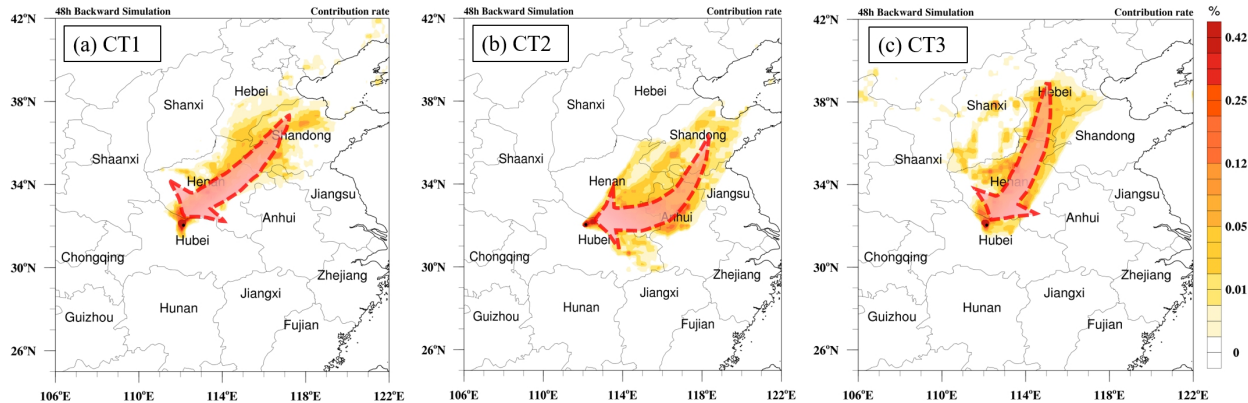
318

Overall, with the southward cold air movement during the season of East Asian winter monsoon, PM<sub>2.5</sub>-rich air mass from the NCP and YRD over CEC was along three main regional transport routes to the THB for the regional HPEs with northerly northeasterly and easterly directions, respectively, basically governed by three patterns of synoptic circulation over CEC with: 1) weak high pressure to the north (CT3), 2) strong high pressure to the northeast (CT1), and 3) weak high pressure to the east (CT2) to the THB over central China, differing from the unfavorable meteorological conditions with weak winds and thermal inversion layer for the HPEs observed in the other air polluted areas of CEC (Ding et al., 2017; Huang et al., 2018). This study revealed a significant modulation of synoptic circulation for regional transport of air pollutants in air quality change.

### **3.5 Contributions of regional PM<sub>2.5</sub> transport to HPEs under three types of synoptic circulation**

Given that three synoptic circulation types CT1, CT2, and CT3 could govern regional PM<sub>2.5</sub> transport along the northeasterly, easterly and northerly pathways over CEC, we further evaluated the contribution of three regional PM<sub>2.5</sub> transport under three types of synoptic circulation to PM<sub>2.5</sub> concentrations for the wintertime HPEs occurring over the THB over central China with the FLEXPART-WRF model.

By calculating the contribution rates with the Eq. (1), we evaluated the contribution rates of regional PM<sub>2.5</sub> transport from non-local regions to PM<sub>2.5</sub> concentrations over central China under three synoptic circulation types CT1, CT2 and CT3. Figure 6 displayed the three corresponding spatial distributions of contribution to PM<sub>2.5</sub> concentrations for HPEs in the THB. As displayed in Figure 6a, regional transport of PM<sub>2.5</sub> was obviously centered on the northeasterly route from CEC to the THB over central China during CT1. As for CT2, the easterly pathway of regional transport was clearly recognized with the high PM<sub>2.5</sub> contribution rates from the YRD to the THB over the CEC (Fig. 6b). Along the northerly regional transport pathway of PM<sub>2.5</sub>, high PM<sub>2.5</sub> sourced from the NCP could enhance air pollution levels for HPEs over central China during CT3 (Fig. 6c).



346

347 **Figure 6.** Distribution of contribution rates (color contours) to surface PM<sub>2.5</sub> over the THB in three major  
 348 pathways (red dash arrows) of regional PM<sub>2.5</sub> transport over CEC under three synoptic circulation types (a)  
 349 CT1, (b) CT2, and (c) CT3 during the wintertime HPEs in the THB from 2015 to 2019 simulated by the  
 350 FLEXPART-WRF model.

351

352 Besides, the contributions of regional transport from non-local regions over CEC to PM<sub>2.5</sub>  
 353 pollution over the THB in central China under CT1, CT2, and CT3 were estimated by using Eq.  
 354 (2). As shown in Table 1, regional PM<sub>2.5</sub> transport contributed 56.7%, 53.9%, and 76.0% to  
 355 surface PM<sub>2.5</sub> in the HPEs over central China during CT1, CT2, and CT3 respectively, indicating  
 356 the dominance of regional PM<sub>2.5</sub> transport modulated by large-scale synoptic circulation in  
 357 enhancing PM<sub>2.5</sub> levels for HPEs over central China, which could have an implication for  
 358 regional joint control on air pollution over CEC (Bai et al., 2021; Shen et al., 2020a).

359

360 **Table 1.** Averaged contribution rates of regional PM<sub>2.5</sub> transport and local emissions over the THB in central  
 361 China under three synoptic circulation types CT1, CT2 and CT3.

Contribution rates	CT1	CT2	CT3
Regional transport	56.7%	53.9%	76.0%
Local emissions	43.3%	46.1%	24.0%

362

363

364 **4 Conclusions**

365 In the present study, we characterized heavy air pollution driven by regional transport of  
366 PM<sub>2.5</sub> occurring in central China, explored the large-scale synoptic circulation influencing  
367 regional PM<sub>2.5</sub> transport with corresponding contributions to PM<sub>2.5</sub> concentrations during the  
368 HPEs from 2015 to 2019 through the analyses of meteorological and environmental observations,  
369 T-mode principal component method (T-PCA) combined with the K-means cluster, and  
370 FLEXPART–WRF model simulations.

371 Approximately 65.2% of the HPEs in the THB over central China were triggered by  
372 regional transport of PM<sub>2.5</sub> over CEC. Based on simulations of the FLEXPART–WRF model,  
373 regional transport of PM<sub>2.5</sub> was centered along three routes in the northerly, northeasterly and  
374 easterly directions respectively. In addition, regional PM<sub>2.5</sub> transport quantitatively contributed  
375 60.2% to PM<sub>2.5</sub> concentrations to HPEs in the THB over central China from 2015 to 2019,  
376 presenting regional PM<sub>2.5</sub> transport in aggravating air pollution levels over central China from a  
377 long-term perspective.

378 The southward invasion of cold air was the vital driving factor for transporting PM<sub>2.5</sub> from  
379 upwind regions over the CEC to the HPEs in central China, which is closely related to the  
380 evolution of synoptic circulation. By using T-mode principal component analysis (T-PCA)  
381 combined with the K-means cluster method, we identified three synoptic circulation types: 1)  
382 strong high pressure to the northeast, 2) weak high pressure to the east, and 3) weak high  
383 pressure to the north that builded three regional PM<sub>2.5</sub> transport routes to central China in the  
384 northeasterly, easterly, and northerly directions with the PM<sub>2.5</sub> contributions of 56.7%, 53.9%,  
385 and 76.0% to the HPEs, respectively, revealing an important effect of large-scale atmospheric  
386 circulations on regional transport of PM<sub>2.5</sub> causing HPEs over central China.

387 Possible uncertainties could exist in this study without consideration the regional transport  
388 of gaseous precursors of PM<sub>2.5</sub> during HPEs and with the classification of synoptic patterns with  
389 sea level pressure. Long-term observation data and comprehensive models of environment and  
390 meteorology could improve our understanding of regional air pollutant transport regulated by  
391 large-scale atmospheric circulation on atmospheric environment change.

392

393

394

395 **Competing interests:** The authors declare that they have no conflicts of interest.

396 **Acknowledgement:** This study was jointly funded by the National Natural Science Foundation  
397 of China (42075186; 41830965; 91744209).

398 **Data availability statement:** The meteorology inputs for WRF model and T-PCA with K-means  
399 cluster are available from NCAR (<https://rda.ucar.edu/datasets/ds083.2/index.html#sf01-wl-/data/ds083.2?g=2>) and ECMWF (<https://cds.climate.copernicus.eu/cdsapp#!/dataset/reanalysis-era5-single-levels?tab=form>) respectively. The hourly meteorological data is sourced from  
400 <http://data.cma.cn/>. The hourly PM<sub>2.5</sub> data are acquired from National Air Quality Monitoring  
401 Network operated by the Ministry of Ecology and Environment of China  
402 (<http://106.37.208.233:20035/>). The data of Multi-resolution Emission Inventory for China was  
403 from <http://www.meicmodel.org/>.

406

407 **References**

- 408 Agarwal, N. K., Sharma, P., & Agarwal, S. K. (2017), Particulate matter air pollution and cardiovascular  
409 disease. *Medicine Science*, 21, 270-279. doi:10.1161/cir.0b013e3181dbece1
- 410 Bai, Y., Zhao, T., Zhou, Y., Kong, S., Hu, W., Xiong, J., Liu, L., Zheng, H., & Meng, K. (2021), Aggravation  
411 effect of regional transport on wintertime PM<sub>2.5</sub> over the middle reaches of the Yangtze River under  
412 China's air pollutant emission reduction process. *Atmospheric Pollution Research*, 12(7), 101111. doi:  
413 10.1016/j.apr.2021.101111
- 414 Bei, N., Li, G., Huang, R., Cao, J., Meng, N., Feng, T., Liu, S., Zhang, T., Zhang, Q., & Molina, L. (2016),  
415 Typical synoptic situations and their impacts on the wintertime air pollution in the Guanzhong basin,  
416 China. *Atmospheric Chemistry and Physics*, 16, 7373–7387. doi:10.5194/acp-2015-710
- 417 Bei, N., Li, X., Tie, X., Zhao, L., Wu, J., Li, X., Liu L., Shen Z., & Li G. (2020), Impact of synoptic patterns  
418 and meteorological elements on the wintertime haze in the Beijing-Tianjin-Hebei region, China from  
419 2013 to 2017. *Science of the Total Environment*, 704, 12. doi: 10.1016/j.scitotenv.2019.135210
- 420 Bi, J., Huang, J., Holben, B., & Zhang, G. (2016), Comparison of key absorption and optical properties  
421 between pure and transported anthropogenic dust over East and Central Asia. *Atmospheric Chemistry and*  
422 *Physics*, 16, 15501–15516. doi:10.5194/acp-16-15501-2016
- 423 Brioude, J., Arnold, D., Stohl, A., Cassiani, M., Morton, D., Seibert, P., Angevine, W., Evan, S., Dingwell, A.,  
424 Fast, J. D., Easter, R. C., Pisso, I., Burkhardt, J., & Wotawa, G. (2013), The Lagrangian particle dispersion

- 425 model FLEXPART-WRF version 3.1. *Geoscientific Model Development*, 6, 1889–1904.  
426 doi:10.5194/gmd-6-1889-2013
- 427 Cai, W., Li, K., Liao, H., Wang, H., & Wu, L. (2017), Weather conditions conducive to Beijing severe haze  
428 more frequent under climate change. *Nature Climate Change*, 7, 257–262. doi:10.1038/nclimate3249
- 429 Che, H., Xia, X., Zhao, H., Dubovik, O., Holben, B. N., Goloub, P., Cuevas-Agulló, E., Estelles, V., Wang, Y.,  
430 Zhu, J., Qi, B., Gong, W., Yang, H., Zhang, R., Yang, L., Chen, J., Wang, H., Zheng, Y., Gui, K., Zhang,  
431 X. C., & Zhang X. Y. (2019), Spatial distribution of aerosol microphysical and optical properties and  
432 direct radiative effect from the China Aerosol Remote Sensing Network. *Atmospheric Chemistry and*  
433 *Physics*, 19, 11843–11864. doi:10.5194/acp-2019-405
- 434 Chen, S., Zhou, G., & Zhu, B. (2017), A method for fast quantification of air pollutant sources. *Acta Scientiae*  
435 *Circumstantiae* (in Chinese), 37, 2474–2481. doi:10.13671/j.hjkxxb.2017.0045
- 436 Chen, Z., Cai, J., Gao, B., Xu, B., Dai, S., He, B., & Xie, X. (2017). Detecting the causality influence of  
437 individual meteorological factors on local PM<sub>2.5</sub> concentrations in the Jing-Jin-Ji region. *Scientific Report*,  
438 7, 40735. doi:10.1038/srep40735
- 439 Chen, Z., Xie, X., Cai, J., Chen, D., Gao, B., He, B., Cheng, N., & Xu, B. (2018), Understanding  
440 meteorological influences on PM<sub>2.5</sub> concentrations across China: a temporal and spatial perspective.  
441 *Atmospheric Chemistry and Physics*, 18, 5343–5358. doi:10.5194/acp-18-5343-2018
- 442 Chou, M., Suarez, M., Ho, C., Yan, M., & Lee, K. (1998). Parameterizations for Cloud Overlapping and  
443 Shortwave Single-Scattering Properties for Use in General Circulation and Cloud Ensemble Models.  
444 *Journal of Climate*, 11, 202–214. doi: 10.1175/1520-0442(1998)011<0202:PFCOAS>2.0.CO;2.
- 445 China State Council: Action Plan on Prevention and Control of Air Pollution, China State Council, Beijing,  
446 China, available at:[http://www.gov.cn/zwgk/2013-09/12/content\\_2486773.htm](http://www.gov.cn/zwgk/2013-09/12/content_2486773.htm) (last access: 06 May  
447 2021), 2013.
- 448 Comrie, A. C., & Yarnal, B. (1992), Relationships between synoptic-scale atmospheric circulation and ozone  
449 concentrations in metropolitan Pittsburgh, Pennsylvania. *Atmospheric Environment*, 26, 301–312.  
450 doi:10.1016/0957-1272(92)90006-E
- 451 Dang, R., & Liao, H. (2019), Severe winter haze days in the Beijing–Tianjin–Hebei region from 1985 to 2017  
452 and the roles of anthropogenic emissions and meteorology. *Atmospheric Chemistry and Physics*, 19(16),  
453 10, 801–10,816. doi:10.5194/acp-19-10801-2019
- 454 Demuzere, M., Trigo, R.M., Vila-Guerau de Arellano, J., & van Lipzig, N.P.M. (2009), The impact of weather  
455 and atmospheric circulation on O<sub>3</sub> and PM<sub>10</sub> levels at a rural mid-latitude site. *Atmospheric Chemistry and*  
456 *Physics*, 9, 2695–2714. doi: 10.5194/acp-9-2695-2009
- 457 Ding, Y. (1993), Monsoons over china, *Springer Science & Business Media*.
- 458 Ding, Y., Wu, P., Liu, Y., & Song, Y. (2017), Environmental and Dynamic Conditions for the Occurrence of  
459 Persistent Haze Events in North China. *Engineering*, 3, 266–271, doi:10.1016/j.eng.2017.01.009

- 460 Fan, H., Zhao, C., & Yang, Y. (2020), A comprehensive analysis of the spatio-temporal variation of urban air  
461 pollution in China during 2014-2018. *Atmospheric Environment*, 220, 117066.  
462 doi:10.1016/j.atmosenv.2019.117066.
- 463 Fast, J. D. & Easter, R. C. (2006), A Lagrangian particle dispersion model compatible with WRF, *7th WRF*  
464 *Users Workshop, NCAR*, 19–22.
- 465 Gui, K., Che, H., Wang, Y., Wang, H., Zhang, L., Zhao, H., Zheng, Y., Sun, T., & Zhang, X. (2019), Satellite-  
466 derived PM<sub>2.5</sub> concentration trends over Eastern China from 1998 to 2016: Relationships to emissions and  
467 meteorological parameters. *Environmental Pollution*, 247, 1125–1133. doi:10.1016/j.envpol.2019.01.056
- 468 Guo, H., Wang, Y., & Zhang, H. (2017), Characterization of criteria air pollutants in Beijing during 2014–  
469 2015. *Environmental Research*, 154, 334–344. doi:10.1016/j.envres.2017.01.029
- 470 He, J., Wu, L., Mao, H., Liu, H., Jing, B., Yu, Y., Ren, P., Feng, C., & Liu, X. (2016), Development of a  
471 vehicle emission inventory with high temporal–spatial resolution based on NRT traffic data and its impact  
472 on air pollution in Beijing—Part 2: impact of vehicle emission on urban air quality. *Atmospheric Chemistry*  
473 and Physics, 16, 3171–3184. doi:10.5194/acp-16-3171-2016
- 474 He, J., Gong, S., Yu, Y., Yu, L., Wu, L., Mao, H., Song, C., Zhao, S., Liu, H., Li, X., & Li, R. (2017a), Air  
475 pollution characteristics and their relationship to meteorological conditions during 2014–2015 in Chinese  
476 major cities. *Environmental Pollution*, 223, 484–496. doi:10.1016/j.envpol.2017.01.050
- 477 He, J., Gong, S., Liu, H., An, X., Yu, Y., Zhao, S., Wu, L., Song, C., Zhou, C., Wang, J., Yin, C., & Yu, L.  
478 (2017b), Influences of meteorological conditions on interannual variations of particulate matter pollution  
479 during winter in the Beijing–Tianjin–Hebei area. *Journal of Meteorological Research*, 31(6), 1062–1069.  
480 doi:10.1007/s13351-017-7039-9
- 481 He, J., Gong, S., Zhou, C., Lu, S., Wu, L., Chen, Y., Ye, Y., Zhao, S., Yu, L., & Yin, C. (2018), Analyses of  
482 winter circulation types and their impacts on haze pollution in Beijing. *Atmospheric Environment*, 192,  
483 94–103. doi:10.1016/j.atmosenv.2018.08.060
- 484 Hu, J., Li, Y., Zhao, T., Liu, J., Hu, X., Liu, D., Jiang, Y., Xu, J., & Chang, L. (2018), An important mechanism  
485 of regional O<sub>3</sub> transport for summer smog over the Yangtze River Delta in eastern China. *Atmospheric*  
486 *Chemistry and Physics*, 18(22), 16239–16251. doi:10.5194/acp-18-16239-2018
- 487 Hu, W., Zhao, T., Bai, Y., Kong, S., Xiong, J., Sun, X., Yang, Q., Gu, Y., & Lu, H. (2021), Importance of  
488 regional PM<sub>2.5</sub> transport and precipitation washout in heavy air pollution in the Twain-Hu Basin over  
489 Central China: Observational analysis and WRF-Chem simulation. *Science of the Total Environment*,  
490 143710. doi:10.1016/j.scitotenv.2020.143710
- 491 Hu, W., Zhao, T., Bai, Y., Shen, L., Sun, X., & Gu, Y. (2020), Contribution of Regional PM<sub>2.5</sub> Transport to Air  
492 Pollution Enhanced by Sub-Basin Topography: A Modeling Case over Central China. *Atmosphere*, 11(11).  
493 doi: 10.3390/atmos11111258, 2020.
- 494 Huang, Q., Cai, X., Wang, J., Song, Y., & Zhu, T. (2018), Climatological study of the Boundary-layer air

- 495 Stagnation Index for China and its relationship with air pollution. *Atmospheric Chemistry and Physics*,  
496 18, 7573–7593. doi:10.5194/acp-18-7573-2018
- 497 Huang, X., Ding, A., Wang, Z., Ding, K., Gao, J., Chai, F., & Fu, C. (2020), Amplified transboundary transport  
498 of haze by aerosol-boundary layer interaction in China. *Nature Geoscience*, 13, 428-434.  
499 doi:10.1038/s41561-020-0583-4
- 500 Huth, R. (1996), An intercomparison of computer-assisted circulations classification methods. *International*  
501 *Journal of Climatology*, 16, 893–922. doi:10.1002/(SICI)1097-0088(199608)16:8<893::AID-  
502 JOC51>3.0.CO;2-Q
- 503 Huth, R., Beck, C., Philipp, A., Demuzere, M., Ustrnul, Z., Cahynová, M., Kyselý, J., & Tveito OE. (2008),  
504 Classifications of atmospheric circulation patterns: Recent advances and applications. *Annals, New York*  
505 *Academy of Sciences*, 1146, 105–152. doi: 10.1196/annals.1446.019
- 506 Hong, S., Noh, Y., & Dudhia, J. (2006), A New Vertical Diffusion Package with an Explicit Treatment of  
507 Entrainment Processes. *Monthly Weather Review*, 134, 2318–2341. doi:10.1175/MWR3199.1
- 508 Hou, X., Zhu, B., Kumar, K. R., de Leeuw, G., Lu, W., Huang, Q., & Zhu, X. (2020), Establishment of  
509 conceptual schemas of surface synoptic meteorological situations affecting fine particulate pollution  
510 across eastern China in the winter. *Journal of Geophysical Research-Atmospheres*, 125, e2020JD033153.  
511 doi:10.1029/2020JD033153
- 512 Kalkstein, L. S., & Corrigan, P. (1986) A synoptic climatological approach for geographical analysis:  
513 Assessment of sulfur dioxide concentrations. *Annals of the Association of American Geographers*, 76,  
514 381–395. doi:10.1111/j.1467-8306.1986.tb00126.x
- 515 Li, J., Liao, H., Hu, J., & Li, N. (2019), Severe particulate pollution days in China during 2013–2018 and the  
516 associated typical weather patterns in Beijing-Tianjin-Hebei and the Yangtze River Delta regions.  
517 *Environmental Pollution*, 248, 74–81. doi:10.1016/j.envpol.2019.01.124
- 518 Li, X., Hu, X.M., Ma, Y., Wang, Y., Li, L., & Zhao, Z. (2019), Impact of planetary boundary layer structure on  
519 the formation and evolution of air-pollution episodes in Shenyang, Northeast China. *Atmospheric*  
520 *Environment*, 214, 116850. doi:10.1016/j.atmosenv.2019.116850
- 521 Lin, Y., Farley, R., & Orville, H. (1983), Bulk Parameterization of the Snow Field in a Cloud Model. *Journal*  
522 *of Applied Meteorology and Climatology*, 22(6), 1065–1092. doi:10.1175/1520-  
523 0450(1983)022<1065:BPOTSF>2.0.CO;2
- 524 Lu, H., Ma, C., Zhao, T., Meng, K., Zheng, X., Li, J., Lu, P., & Liu, H. (2021), Analysis of synoptic pattern on

- 525 PM<sub>2.5</sub> heavy pollution over the Beijing-Tianjin-Hebei region in winter based on PCT. *Acta Scientiae  
526 Circumstantiae* (in Chinese), 41(3), 898-904. doi:10.13671/j.hjkxxb.2020.0532
- 527 Liao, Z., Xie, J., Fang, X., Wang, Y., Zhang, Y., Xu, X., & Fan, S. (2020), Modulation of synoptic circulation  
528 to dry season PM<sub>2.5</sub> pollution over the Pearl River Delta region: An investigation based on self-  
529 organizing maps. *Atmospheric Environment*, 230, 117482. doi:10.1016/j.atmosenv.2020.117482
- 530 Liu, Y., He, J., Lai, X., Zhang, C., & Che, H. (2020), Influence of atmospheric circulation on aerosol and its  
531 optical characteristics in the pearl river delta region. *Atmosphere*, 11(3), 288.  
532 doi:10.3390/atmos11030288
- 533 Mlawer, E., Taubman, S., Brown, P., Iacono, M., & Clough, S. (1997), Radiative transfer for inhomogeneous  
534 atmospheres: RRTM, a validated correlated-k model for the longwave. *Journal of Geophysical  
535 Research- Atmospheres*, 102(D14), 16663–16682. doi:10.1029/97jd00237
- 536 Miao, Y., Guo, J., Liu, S., Liu, H., Li, Z., Zhang, W., & Zhai, P. (2017), Classification of summertime synoptic  
537 patterns in Beijing and their associations with boundary layer structure affecting aerosol pollution.  
538 *Atmospheric Chemistry and Physics*, 17, 3097–3110. doi:10.5194/acp-17-3097-2017
- 539 Ning, G., Yim, S.H.L., Wang, S., Duan, B., Nie, C., Yang, X., Wang, J., & Shang, K. (2019), Synergistic effects  
540 of synoptic weather patterns and topography on air quality: a case of the Sichuan Basin of China.  
541 *Climate Dynamics*, 53, 6729–6744. doi:10.1007/s00382-019-04954-3
- 542 Ren, Y., Zheng, S., Wei, W., Wu, B., Zhang, H., Cai, X., & Song, Y. (2018), Characteristics of turbulent  
543 transfer during episodes of heavy haze pollution in Beijing in Winter 2016/17. *Journal of  
544 Meteorological Research*, 32(1), 69–80. doi: 10.1007/s13351-018-7072-3
- 545 Shahgedanova, M., Burt, T., & Davies, T. (1998), Synoptic climatology of air pollution in Moscow. *Theoretical  
546 and Applied Climatology*, 61, 85–102. doi:10.1007/s007040050054
- 547 Shen, L., Zhao, T., Wang, H., Liu, J., Bai, Y., Kong, S., Zheng, H., Zhu, Y., & Shu, Z. (2020a), Importance of  
548 meteorology in air pollution events during the city lockdown for COVID-19 in Hubei Province, Central  
549 China. *Science of the Total Environment*, 754, 142227. doi:10.1016/j.scitotenv.2020.142227
- 550 Shen, L., Wang, H., Zhao, T., Liu, J., Bai, Y., Kong, S., & Shu, Z. (2020b), Characterizing regional aerosol  
551 pollution in Central China based on 19 years of MODIS data: Spatiotemporal variation and aerosol type  
552 discrimination. *Environmental Pollution*, 263, 114556. doi:10.1016/j.envpol.2020.114556
- 553 Shu, Z., Liu Y., Zhao, T., Xia, J., Wang, C., Cao, L., Wang, H., Zhang, L., Zheng, Y., Shen, L., Luo, L., & Li, Y.  
554 (2021), Elevated 3D structures of PM<sub>2.5</sub> and impact of complex terrain-forcing circulations on heavy

- 555 haze pollution over Sichuan Basin, China. *Atmospheric Chemistry and Physics*, 21(11), 9253–9268. doi:  
556 10.5194/acp-21-9253-2021
- 557 Skamarock, W. C., Klemp, J. B., Dudhia, J., Gill, D. O., Barker, D. M., Duda, M., Huang, X.-Y., Wang, W., &  
558 Powers, J. G. (2008), A Description of the Advanced Research WRF Version 3, NCAR Technical Note,  
559 Boulder, CO, USA. doi:10.13140/RG.2.1.2310.6645
- 560 Stohl, A., Forster, C., Frank, A., Seibert, P., & Wotawa, G. (2005), Technical note: The Lagrangian particle  
561 dispersion model FLEXPART version 6.2. *Atmospheric Chemistry and Physics*, 5, 2461 – 2474,  
562 doi:10.5194/acp-5-2461-2005
- 563 Su, W., Liu, C., Hu, Q., Zhao, S., Sun, Y., Wang, W., Zhu, Y., Liu, J., & Kim, J. (2019), Primary and secondary  
564 sources of ambient formaldehyde in the Yangtze River Delta based on ozone mapping and profiler suite  
565 (OMPS) observations. *Atmospheric Chemistry and Physics*, 19, 6717–6736. doi:10.5194/acp-19-6717-  
566 2019
- 567 Wang, X., & Zhang, R. (2020), Effects of atmospheric circulations on the interannual variationin PM<sub>2.5</sub>  
568 concentrations over the Beijing–Tianjin–Hebei region in 2013–2018, *Atmospheric Chemistry and Physics*,  
569 20, 7667–7682. doi:10.5194/acp-20-7667-2020
- 570 Wang, Q., Fang, J., Shi, W., & Dong, X. (2020), Distribution characteristics and policy-related improvements  
571 of PM<sub>2.5</sub> and its components in six Chinese cities, *Environmental Pollution*, 266.  
572 doi:10.1016/j.envpol.2020.115299
- 573 Yan, Y., Zhou, Y., Kong, S., Lin, J., Wu, J., Zheng, H., Zhang, Z., Bai., Y, Ling, Z., Liu, D., & Zhao, T. (2020)  
574 Effectiveness of emission control to reduce PM<sub>2.5</sub> pollution of Central China during winter haze episodes  
575 under various potential synoptic controls. *Atmospheric Chemistry and Physics*. doi:10.5194/acp-2020-920
- 576 Yu, C., Zhao, T., Bai, Y., Zhang, L., Kong, S., Yu, X., He, J., Cui, C., Yang, J., You, Y., Ma, G., Wu, M., &  
577 Chang, J. (2020), Heavy air pollution with a unique “non-stagnant” atmospheric boundary layer in the  
578 Yangtze River middle basin aggravated by regional transport of PM<sub>2.5</sub> over China, *Atmospheric  
579 Chemistry and Physics*, 20, 7217-7230. doi: 10.5194/acp-20-7217-2020
- 580 Zhang, H., Yuan, H., Liu, X., Yu, J., & Jiao, Y. (2018), Impact of synoptic weatherpatterns on 24 h-average  
581 PM<sub>2.5</sub> concentrations in the North China Plain during 20132-017, *Science of the Total Environment*, 627,  
582 200-210. doi: 10.1016/j.scitotenv.2018.01.248
- 583 Zhang, J., Zhu, T., Zhang, Q., Li, C., Shu, H., Ying, Y., Dai, Z, Wang, X., Liu, X., Liang, A, Shen, H., & Yi, B.  
584 (2012), The impact of circulation patterns on regional transport pathways and air quality over Beijing and  
585 its surroundings. *Atmospheric Chemistry and Physics*, 12, 5031–5053, doi: 10.5194/acp-12-5031-2012

- 586 Zhang, K., Zhao, C., Fan, H., Yang, Y., & Sun, Y. (2019), Toward Understanding the Differences of PM<sub>2.5</sub>  
587 Characteristics Among Five China Urban Cities. *Asia-Pacific Journal of Atmospheric Sciences*, 1–10,  
588 doi:10.1007/S13143-019-00125-W
- 589 Zhang, Q., Zheng, Y., Tong, D., Shao, M., Wang, S., Zhang, Y., Xu, X., Wang, J., He, H., & Liu, W. (2019),  
590 Drivers of improved PM<sub>2.5</sub> air quality in China from 2013 to 2017. *Proceedings of the National Academy  
591 of Sciences*, 116, 24463–24469. doi:10.1073/pnas.1907956116
- 592 Zhang, Q., Quan, J., Tie, X., Li, X., Liu, Q., Gao, Y., & Zhao, D. (2015), Effects of meteorology and  
593 secondary particle formation on visibility during heavy haze events in Beijing, China. *Science of the Total  
594 Environment*, 502, 578–584, doi:10.1016/j.scitotenv.2014.09.079
- 595 Zhang, Q., Song, Y., Li, M., & Zheng, B. (2020), Anthropogenic Emissions of SO<sub>2</sub>, NO<sub>x</sub>, and NH<sub>3</sub> in China,  
596 in: Atmospheric Reactive Nitrogen in China: Emission, Deposition and Environmental Impacts, edited by:  
597 Liu, X. and Du, E., *Springer Singapore*, 13–40, doi:10.1007/978-981-13-8514-8\_2
- 598 Zhang, R., Li, Q., & Zhang, R. (2013), Meteorological conditions for the persistent severe fog and haze event  
599 over eastern China in January 2013. *Science China Earth Sciences*, 57, 26–35. doi:10.1007/s11430-013-  
600 4774-3
- 601 Zhang, Y., Ding, A., Mao, H., Nie, W., Zhou, D., Liu, L., Huang, X., & Fu, C. (2016), Impact of synoptic  
602 weather patterns and inter-decadal climate variability on air quality in the North China Plain during 1980–  
603 2013. *Atmospheric Environment*, 124, 119–128. doi: 10.1016/j.atmosenv.2015.05.063
- 604 Zhou, X., Bei, N., Liu, H., Cao, J., Xing, L., Lei, W., Molina, L.T., & Li, G. (2017), Aerosol effects on the  
605 development of cumulus clouds over the Tibetan Plateau. *Atmospheric Chemistry and Physics*, 17(12),  
606 7423–7434. doi: 10.5194/acp-17-7423-2017
- 607 Zhu, W., Xu, X., Zheng, J., Yan, P., Wang, Y., & Cai, W. (2018), The characteristics of abnormal wintertime  
608 pollution events in the Jing-Jin-Ji region and its relationships with meteorological factors, *Science of the  
609 Total Environment*, 626, 887–898. doi:10.1016/j.scitotenv.2018.01.083
- 610 Zhu, Y., Zhao T., Bai, Y., Xu, J., Sun, X., Hu, W., Chang J., Yang J., & Zhu, C. (2021), Characteristics of  
611 Atmospheric Particulate Matter Pollution and the Unique Wind and Underlying Surface Impact in the  
612 Twain-Hu Basin in Winter. *Environmental Science* (in Chinese). doi:10.13227/j.hjkx.202103050.
- 613 Zhong, J., Zhang, X., Wang, Y., Wang, J., Shen, X., Zhang, H., Wang, T., Xie, Z., Liu, C., Zhang, H., Zhao, T.,  
614 Sun, J., Fan, S., Gao, Z., Li, Y., & Wang, L. (2019), The two-way feedback mechanism between  
615 unfavorable meteorological conditions and cumulative aerosol pollution in various haze regions of China.  
616 *Atmospheric Chemistry and Physics*, 19(5), 3287-3306. doi: 10.5194/acp-19-3287-2019
- 617 Zhong, Q., Ma, J., Shen, G., Shen, H., Zhu, X., Yun, X., Meng, W., Cheng, H., Liu, J., Li, B., Wang, X., Zeng,  
618 E. Y., Guan, D., & Tao, S. (2018), Distinguishing Emission-Associated Ambient Air PM<sub>2.5</sub>  
619 Concentrations and Meteorological Factor-Induced Fluctuations. *Environmental Science & Technology*,  
620 52. doi:10.1021/acs.est.8b02685

- 621 Zong, L., Yang, Y., Gao, M., Wang, H., Wang, P., Zhang, H., Wang, L., Ning, G., Liu, C., Li, Y., & Gao., Z.  
622 (2021), Large-scale synoptic drivers of co-occurring summertime ozone and PM<sub>2.5</sub> pollution in eastern  
623 China. *Atmospheric Chemistry and Physics*, 21(11), 9105-9124. doi:10.5194/acp-21-9105-2021